Journal of Photochemistry & Photobiology, A: Chemistry 434 (2023) 114235

Contents lists available at ScienceDirect

Journal of Photochemistry & Photobiology, A: Chemistry

journal homepage: www.elsevier.com/locate/jphotochem

Photocatalytic abatement of air pollutants: Focus on their interference in mixtures

Radek Zouzelka [a,b,*], Ivana Martiniakova [a,b], Tomas Duchacek [b], Barbora Muzikova [a], Eliska Mikyskova [a], Jiri Rathousky [a,*]

[a] J. Heyrovsky Institute of Physical Chemistry of the CAS, Center for Innovation in the Field of Nanomaterials and Nanotechnologies, Dolejskova 3, Prague 18223, Czech Republic

[b] Advanced Materials – JTJ s.r.o., Kamenne Zehrovice 23, Kamenne Zehrovice 273 01, Czech Republic

ARTICLE INFO

Keywords:
Photocatalysis
TiO_2
NO_x
Acetaldehyde
Ozone
Mixtures

ABSTRACT

Up to now, the research has been mostly devoted to the photocatalytic removal of individual pollutants. As in real situations, the pollutants are always presented in a mixture, it is crucial to know whether there is some sort of interference, which can influence the efficiency of the whole photocatalytic degradation process. Here, we investigated the ability of two commercial coatings (binder-containing FN NANO®2 and binder-free AEROXIDE® TiO_2 P25) to abate ozone, nitric oxide, and acetaldehyde separately and in their mixtures. Both photocatalysts effectively removed the pollutants present separately in the air stream, achieving conversions of 30–60 % (at an inlet concentration of 0.1 ppmv), even at the UV-A irradiation intensity as low as 0.05 mW cm^{-2}. Furthermore, the use of binder-containing coating provided stable ozone conversions (30–40 %) in the full range of relative humidity, which is extraordinary in comparison with published data. The kinetic analysis indicates that the degradation mechanisms of nitric oxide, acetaldehyde, and ozone considerably differed. While for nitric oxide the reaction in the adsorbed state played a crucial role, for acetaldehyde and ozone that was marginal. Importantly, owing to the differences in degradation mechanisms, no mutual interference occurred when pollutant mixtures were treated. This finding is of major importance for the application of photocatalysis as environmental technology.

1. Introduction

Polluted air both outdoors and indoors contains a complex mixture of compounds, whose chemical properties substantially differ. Their most important groups include inorganic oxides (NOx, SOx, CO), volatile organic compounds (VOCs) and ozone.

The major source of NOx in Europe is road transport, producing around 40 % of the total emissions, comprising a mixture of nitric oxide (NO) and nitrogen dioxide (NO_2). European directives impose a limit on NO_2 concentration in ambient air of 40 μg m^{-3} (0.021 ppmv) averaged over 1 year and of 200 μg m^{-3} (0.106 ppmv) averaged over 1 h (Directive 2008/50/EC, 2008), which must not be exceeded on more than 18 occasions each year. However, such limit concentrations are frequently exceeded, especially in large cities with high traffic and industrial areas.

Regards the danger of VOCs, these are among the most abundant chemical pollutants in the indoor environment. The major classes of emitted VOCs are alkanes, alkenes, aromatic hydrocarbons, and oxygenated compounds. They are suspected one of the major causes of sick building syndrome (SBS) associated with a sore throat, headache, or eye irritation that occur when entering a newly constructed or refurbished building [14].

Moreover, in the presence of ultraviolet illumination, VOCs react with NOx and other airborne species forming ground-level ozone. Directive 2002/3/EC of the European Parliament imposes a limit on ozone in ambient air of 120 μg m^{-3} (0.056 ppmv) over 8 h. Ozone is harmful to human health, causing throat dryness, headaches, and damage to mucus membranes, even at low concentration levels of 0.1–1 ppmv [3].

To efficiently remove these pollutants requires a technology whose efficiency is sufficiently high for all of them. Moreover, large volumes of air outside and inside buildings should be treated, which complicates the selection of suitable technology.

Heterogeneous photocatalysis on TiO_2-based coatings offers a

* Corresponding authors.
E-mail address: jiri.rathousky@jh-inst.cas.cz (J. Rathousky).

https://doi.org/10.1016/j.jphotochem.2022.114235
Received 16 June 2022; Received in revised form 4 August 2022; Accepted 20 August 2022
Available online 3 September 2022

sustainable solution. A number of studies have been devoted to the assessment of the effect of relevant process parameters on the efficiency of this process [1,4,10,9].

However, the degradation of mixtures of pollutants has been addressed very rarely, even if in real polluted air practically never only one single pollutant is contained. Therefore, a question arises if and how a mutual interference of the concurrently present pollutants may influence the efficiency of this technology. With respect to this issue, the present study is aimed at.

(i) the elucidation of the differences in the degradation mechanisms of the most important types of air pollutants, and
(ii) explanation of the role of their simultaneous presence on the efficiency of the whole process.

The extensive experimental data and their analysis showed that owing to the differences in their degradation mechanisms, the interference did not practically occur, and the pollutants were degraded as if they were present separately.

2. Materials and methods

2.1. Preparation, characterization, and mechanical performance of the coatings

Water suspension of AEROXIDE® TiO_2 P25 (Evonik Industries, Germany, hereinafter referred to as P25), which served as a photocatalytic standard, was applied on glass substrates (5 × 10 cm in size) using airbrush (PME) spraying (pH of P25 nanoparticles suspended in ultrapure water was 4.7). The deposition time for each layer was very short about one second. After the application of an individual layer, there was a technological break to let the coating dry. In this manner, three layers of P25 coating were sprayed creating a film of 50 mg in weight.

The FN NANO®2 coating (FN-NANO s.r.o., Czech Republic, hereinafter referred as FN2) was applied onto glass supports analogously as the P25 deposition process. FN NANO®2 is a composite photocatalytic coating consisting of TiO_2 P25 (74 %), the rest being an inorganic binder. Detailed information regarding this coating can be found in U.S. patent no. 8,647,565 (2009).

The loading of both coatings onto the 50 cm^2 glass support was 50 mg (1 mg cm^{-2}). However, due to the presence of an inorganic binder, the sample FN2 contained only 37 mg of TiO_2, 13 mg corresponding to the binder. The reason for choosing such loading was due to the recommendation by the manufacturer.

The X-ray diffraction patterns were measured on PANalytical X'Pert PRO diffractometer equipped with Co tube ($\lambda = 0.178901$ nm) using the Bragg-Brentano geometry. The diffraction patterns were evaluated by the Rietveld method [13] using TOPAS 3 software with a fundamental parameter approach [2]. The broadening of the diffraction lines was interpreted only in terms of crystallite sizes, microscopic deformations were neglected. When included, the size of the crystallites would increase by a maximum of 1 nm. For better spectra comparability, the background was removed from the diffraction pattern and the intensity was scaled.

The optical properties of the coatings were measured with a Perkin Elmer Lambda 950 UV–vis-NIR spectrometer equipped with Spectralon and gold integration spheres for diffuse reflectance measurements in the UV-NIR region. The structural-textural properties of P25 and FN2 coatings were detailly discussed by Zouzelka and Rathousky [16].

The surface morphology of the layers was studied using Jeol JEM-2100 UHR transmission electron microscope. The texture properties of the coatings were determined by analysis of adsorption isotherms of nitrogen at ca 77 K performed with 3FLEX (Micromeritics) volumetric adsorption unit.

Spatial heterogeneity in mechanical properties of FN2 and P25 coatings was assessed by means of nanoindentation mapping. Distributions of indentation hardness (H_{IT}) and reduced elastic modulus (E_r) were acquired with Hysitron TI980 Nanoindenter (Bruker Corp.). Indentation map originated from grid of 30x30 indents with separation 3 μm. Indentation load function was set to displacement control feedback mode at peak displacement of 200 nm. Standard diamond 3-sided Berkovich probe was used for nanoindentation. Indentation positions were correlated with an optical view of nanoindenter's light microscope. Microscopy image showed complex morphology of coating as well as suggested presence of different material phases. Mechanically mapped representative areas were approximately 90 μm × 90 μm. Distribution of mechanical properties are used for qualitative comparison of FN2 and P25 samples in this case.

2.2. Photocatalytic testing

The experimental conditions for photocatalytic abatement of NO and acetaldehyde were selected according to the given ISO standards (ISO 22197–1: 2007 and ISO 17168–2:2018) and to their modifications, reflecting the conditions of urban environment. Therefore, the inlet NO concentrations were either 0.1 ppmv (122.6 μg m^{-3}) or 1.0 ppmv (ISO 22197–1:2007; 1226 μg m^{-3}); for acetaldehyde 0.1 ppmv (183 μg m^{-3}), 1.0 ppmv (1830 μg m^{-3}) and 5.0 ppmv (ISO 17168–2:2018; 9150 μg m^{-3}), while for ozone 0.1 ppmv (196 μg m^{-3}).

Testing the photocatalytic activity was performed using the flow reactor recommended by ISO 22197–1:2007. The area of the irradiated photocatalytic surface was 50 cm^2 (5 × 10, in cm), the flow rate of reaction mixture containing pollutant and the linear velocity of the streaming gas being 3000 cm^3 min^{-1} and 0.2 m s^{-1}, respectively. The total volume of air treated in 24 h was 4.32 m^3. As the free volume of the reactor was 80 cm^3 (5 × 32 × 0.5, in cm), the volume per irradiated area was 1.6 cm^3 cm^{-2}.

The concentration of NO_x, VOC and ozone was determined using a set-up of HORIBA analyzers, which included APNA-370 (for the determination of NO, NO_2 and NO_x), APHA-370 (total organic carbon-TOC, CH_4, and non-CH_4) and APOA-370 (O_3).

The day before the photocatalytic experiments, the samples were irradiated overnight by UV-A light of intensity 2.0 mW cm^{-2} in order remove any residual organics from the surface. Just before the experiment itself, the synthetic air containing either nitric oxide, acetaldehyde or ozone was streamed over the sample in dark to achieve an adsorption equilibrium between the gas phase and the sample surface. It took approximately 10 min. Due to this, the photocatalytic removal of each pollutant was solely by photocatalysis, neither by a heterogeneous reaction with titania nor by the pollutant adsorption onto the surface.

After reaching equilibrium, the samples started being irradiated by black-light fluorescent lamps (Philips) in a planar arrangement, emitting a dominant wavelength of 365 nm. The distance between the lamps and the coatings was adjusted to achieve the needed irradiation intensity. The distance between lamp and the samples was 40 cm and the given UV-A intensity was adjusted by the change of the power voltage of the lamp. Concerning the UV-A light intensities at 365 nm, they varied from 0.05 mW cm^{-2} to 5.00 mW cm^{-2}. The reason for choosing such a wide range of light intensities was to simulate the conditions of bright sunny weather (summer in Central Europe) and weather with cloudy skies (winter in Central Europe). Furthermore, the hygienic limit of UV-A intensity (0.05 mW cm^{-2}) applicable for indoor environment was taken into an account. All photocatalytic experiments were performed in triplicate with the data variation less than 10 per cent.

For the evaluation of photocatalytic abatement of inorganic and organic pollutant, different quantities were formulated as follows:

Reaction rate r / $\mu mol\ m^{-2}h^{-1}$ is the number of moles of a given substance degraded in a gas stream within one hour on a photocatalytic surface area of one m^2. If the reaction rate is positive (r) the substance is formed, if negative ($-r$) removed. The reaction rate of the NO_x, VOC and ozone (SFig. 3A, SFig. 3B) removal is more suitable than conversion in

per cent, which cannot be used for the calculation of photocatalytic performance under differing situation, e. g. on a coated external wall. Using moles is more suitable than mass units because of a different molar mass of reactant, intermediates and products.

The reaction rate r is expressed using the Langmuir–Hinshelwood model with the kinetic constant k (in units $\mu mol\ m^{-2}h^{-1}$) and the Langmuir adsorption constant K (in units $m^3/\mu mol$).

The analysis of the kinetic data for acetaldehyde and ozone showed that the Langmuir-Hinshelwood model is not suitable for the description of these reactions due to their negligible sorption. Therefore, for acetaldehyde, a power model with the reaction rate order of 0.5 was used, the unit of the reaction constant k *(TOC)* / $\mu mol^{1/2}\ m^{-1/2}h^{-1}$. For ozone, the 1st order reaction rate showed suitable in the range of concentrations up to 0.125 ppmv, with the unit of the reaction constant k *(Ozone)* equaling m/h.

Photocatalytic uptake coefficient γ is defined as the ratio of the number of collisions leading to reaction and the total number of all collisions [7]. The γ threshold limit value of $1x10^{-5}$ was proposed to ensure sufficient photocatalytic activity (Ifang et al., 2014).

3. Results and discussion

3.1. Physical-chemical properties of the coatings

The structural properties of both photocatalysts, investigated by X-ray diffraction (SFig. 1A), showed that P25 consisted of dominant anatase phase while the presence of rutile was only 12 per cent (Table 1), FN2 containing besides anatase and rutile 13 per cent of inorganic binder.

The diffuse reflectance spectra of the FN2 and P25 coatings exhibited an absorption edge below 400 nm (SFig. 1B). A significant red shift in the absorbance of FN2 provides some evidence of interactions between the binder and TiO_2. Therefore, this material can generate electron-hole pairs upon irradiation with longer wavelength light [6].

High-resolution electron microscopy revealed that FN2 coating is formed of a spongy microstructure due to the inorganic binder, on which TiO_2 particles are attached (SFig. 1C). The binder particles were at least two-times larger compared to the uniform TiO_2. Moreover, the binder was porous, which is in an agreement with the larger surface area calculated from adsorption experiments. Such open-structure of FN2 composite coating offers better accessibility for the polluted air and provides more space for the deposition of potential reaction products, which can suppress the photocatalyst deactivation.

The binder-containing photocatalyst exhibited better mechanical performance, providing very good cohesion and adhesion to the construction material, as documented a two-times higher hardness of the FN2 coatings in comparison with P25 ones (SFig. 1D).

Moreover, due to the presence of binder, the potential release of nanoparticles from such composite structure is virtually impossible. Generally, without any binder, the coated photocatalyst cannot achieve a satisfactory strength and durability when it is deposited. This is an important feature which should be fulfilled regarding the potential adverse effects on human and the environment.

For the detail information of the structural properties, please see our previous study [16] or visit the Supporting information section.

Table 1
Structural and morphological properties of the photocatalytic coatings.

Coating	XRD[a] % Anatase /Rutile/binder	XRD[a] nm Anatase/Rutile/ binder	BET [b] /nm	S_{BET} [b] /m^2 g^{-1}	E_g [c] /eV
FN2	77 / 10 / 13	16 / 22 / 133	nd	82	3.05
P25	88 / 12 / 0	16 / 22 / 0	28	47	3.20

[a]crystallite weight / % and size / nm determined by X-ray diffraction; [b] particles size / nm and specific surface area / $m^2\ g^{-1}$ calculated from nitrogen adsorption isotherms; [c] band gap energy determined by UV/Vis spectroscopy.

3.2. Photocatalytic degradation of pollutants separately

3.2.1. Photolysis, re-use and de-activation

To achieve a valid assessment of the role of photocatalysis itself in the process of pollutant degradation, the extent of photolysis was determined. SFig. 2A shows that all the three pollutants addressed are highly stable even at high intensity of UV light of 5.0 mW cm^{-2}. Therefore, the effect of photolysis on the pollutant degradation can be neglected.

Concerning the applicability of the photocatalytic technology, both the stability of its performance and the re-use possibility are of utmost importance. It was found that there is only a very slight performance decrease on re-use for all three pollutants at typical reaction conditions. The high stability of performance is further proved by long term experiments, which show the reaction rate achieves a stable steady-state value for all three pollutants after about five hours on stream (SFig 2B).

3.2.2. Photocatalytic abatement of nitric oxide

The analysis of the experimental data showed that the dependence of reaction rate on the NO_x concentration can be reasonably modelled using the Langmuir-Hinshelwood mechanism. Consequently, the rate is determined by the values of two model constants, $k(NO_x)$ and $K(NO_x)$. Fig. 1 shows that for FN2 and P25 coatings their absolute values and their variation with the irradiation intensity differed significantly.

The values of the rate constant $k(NO_x)$ are much higher for FN2 (with an exception of the lowest irradiation intensities). In the case of FN2 coating, the reaction rate constant k increased with irradiation intensity, reaching plateau at ca. 300 μmol $m^{-2}h^{-1}$. On that plateau, the rate constant was fourfold higher compared to that of P25, even though the amount of titanium dioxide in the FN2 coating was about 13 per cent lower.

Regarding the adsorption of pollutant on photocatalyst FN2 surface, a significant decrease of $K(NO_x)$ constant values with increasing intensity was observed (Fig. 1A). The reason is a high reaction rate of adsorbed NO molecules with reactive oxidation species (ROS) formed during light absorption. Intensity of 0.25 mW cm^{-2} seems as the threshold-value above which $K(NO_x)$ did not depend on the intensity.

On the other hand, the photocatalytic performance of highly active industry standard P25 showed different behavior (Fig. 1B), both constants being independent on UV-A intensity in the whole region. Reaction rate constant was only 70 μmol $m^{-2}h^{-1}$, which is a characteristic value in the whole intensity region used. A reasonable explanation might be the absence of the beneficial effect of a large surface area (Table 1), large pore volume (SFig. 1C) and the presence of alkaline binder, which all improves the FN2 performance. Fig. 1B clearly shows that for P25 the maximum performance was achieved at the lowest irradiation intensity used (0.05 mW cm^{-2}) and afterwards no increase in activity occurred. It is therefore reasonable to conclude that the reaction rate itself is not a rate-determining step. Probably the mass transport plays a key role.

3.2.3. Photocatalytic abatement of acetaldehyde

The mechanism of the acetaldehyde degradation substantially differs from that of NO. According to the Langmuir-Hinshelwood model, acetaldehyde molecule exhibited negligible adsorption onto surface ($K \sim 0$), and, thus, the determination of reaction rate and adsorption constants by applying of such model was not valid. The photocatalytic reaction seems to occur immediately when the acetaldehyde molecule reaches the surface or in its vicinity, without deposition of any residues. Therefore, we calculated the reaction rate constant according to a power model with the reaction rate order of 0.5 (SFig. 4A). Similar conclusion for photocatalytic degradation of acetone was reported by Zorn and coworkers [15].

The performance of FN2 and P25 coatings was similar, their reaction

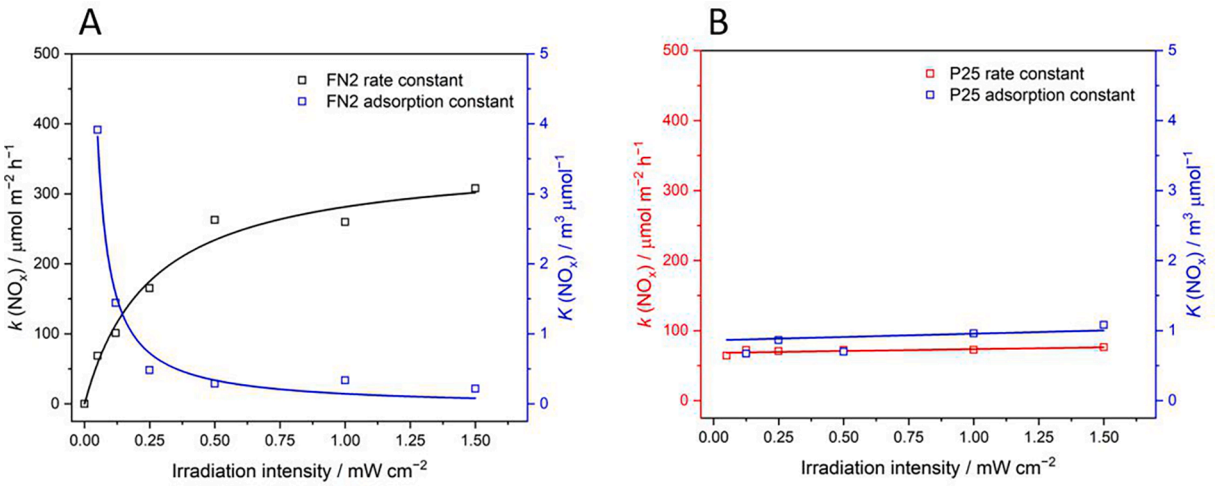

Fig. 1. Apparent reaction rate and adsorption constants of photocatalytic NO_x abatement over FN2 (2A) and P25 (2B) coatings. The data were calculated based on the photocatalytic experiments performed in triplicate with the variation less than 10 per cent.

rate constants *k* (Fig. 2A, B) increased almost linearly and did not reach a plateau with increasing irradiation intensity. Consequently, the features of FN2, which were beneficial for the NO degradation, did not apply.

3.2.4. Photocatalytic abatement of ozone

Fig. 3 shows that FN2 exhibited a better performance than P25, its *k* constant being about two-times higher. The variation in the irradiation intensity had only limited effect on the 1st order reaction rate constant for both photocatalysts, even at intensity as low as 0.05 mW cm^{-2}, significant ozone removal was achieved. Dark experiments showed that the degradation of ozone was only marginal, the effect of heterogeneous photocatalysis being dominant. The higher efficiency of FN2 is probably connected with its open morphology and larger surface area enabling better access of ozone molecules towards the photocatalyst.

Another important superiority of FN2 coating over P25 concerned the effect of the air humidity (Table 2). For FN2 the detrimental effect was only slight in the maximum range of relative humidity. However, the drop of P25 activity was as high as 70 per cent. This feature is of major importance as high humidity is often encountered in real environmental applications.

3.2.5. Degradation mechanisms of individual pollutant

The photocatalytic oxidation of nitric oxide produces nitrogen dioxide, which is subsequently oxidized by the attack of water or OH radicals into the final product, HNO_3. This general conclusion agrees with the observations in the present study, as the final product of photocatalytic oxidation captured on the photocatalytic surfaces was exclusively nitrites () while the concentrations of HONO and were below the detection limit.

As no carbonaceous deposits on the photocatalytic surface were found after the photocatalytic tests, acetaldehyde was exclusively converted to gaseous products. The determination of organic carbon in effluent showed that its concentration was lower than in inlet, therefore, a proportion of acetaldehyde was mineralized. The mineralized amount corresponds to CO_2 formed. Consequently, the concentration of CO_2 could be determined indirectly. Regarding the literature, acetaldehyde can be oxidized to CO_2 directly without additional intermediates being formed. Alternatively, a sequential reaction pathway was proposed, under which acetaldehyde is oxidized to acetic acid, formic acid, and, finally, to CO_2 [5]. The primary difference in these reaction pathways is whether acetic acid is a reaction intermediate or not. According to our observation, the former mechanism seems relevant. The adsorbed species (acetates, formates or corresponding acids) on the photocatalysts surface did not form and acetaldehyde was oxidized directly to carbon dioxide.

The mechanism of photocatalytic removal of ozone over titania

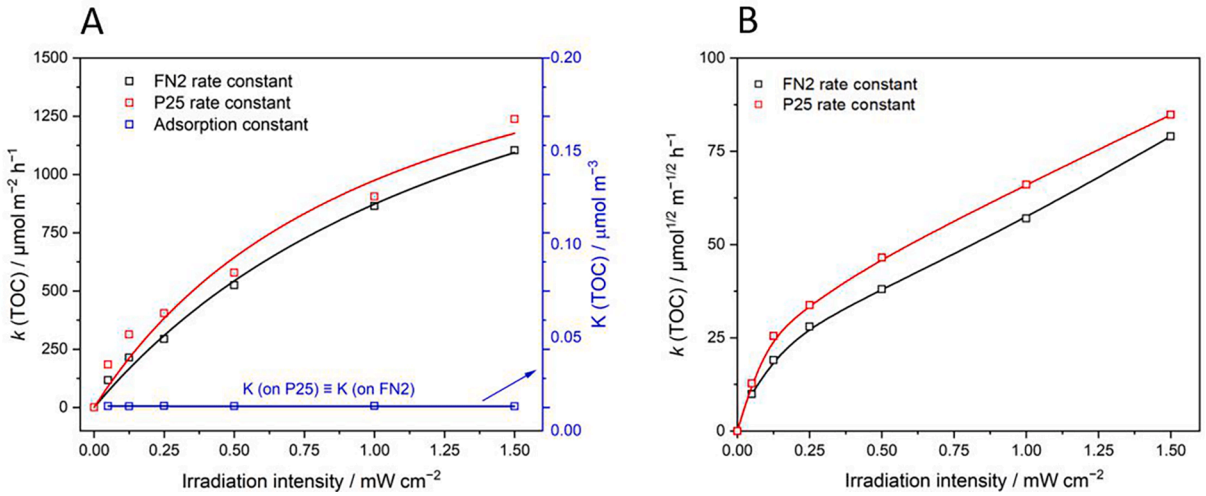

Fig. 2. Apparent reaction rate constant and adsorption constants of photocatalytic acetaldehyde abatement over FN2 and P25 coatings. Reaction rate-order of 1.0 (A) and 0.5 (B). The data were calculated based on the photocatalytic experiments performed in triplicate with the variation less than 10 per cent.

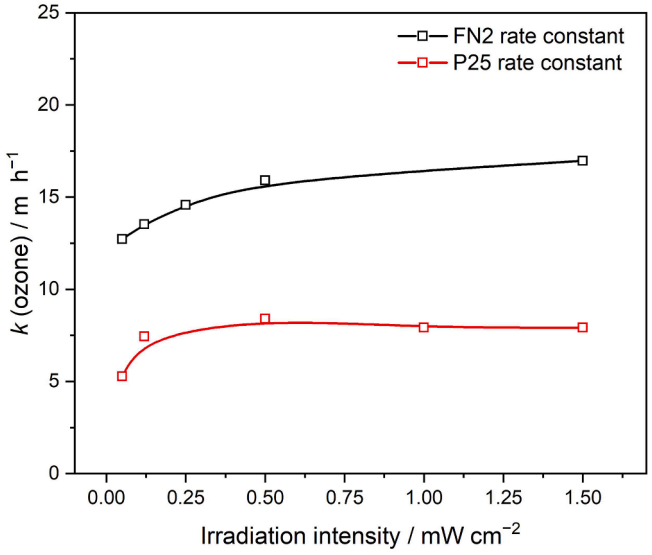

Fig. 3. Apparent reaction rate constants of photocatalytic ozone abatement over FN2 and P25 coatings. The data were calculated based on the photocatalytic experiments performed in triplicate with the variation less than 10 per cent.

Table 2
Photocatalytic removal of ozone in the air stream with various relative humidity. The inlet ozone concentration was 0.1 ppmv.

Relative humidity / %	FN2 Conversion / %	P25 Conversion / %
0	42	42
50	40	33
100	33	13

surface is suggested so that Ti^{4+} is reduced to Ti^{3+} by a photoinduced electron, which is a site for ozone decomposition forming O_3^- [8]. This anion may subsequently react with water producing O_2. On the other hand, the formation of another ozone ion O_4^- is feasible *via* oxidation of ozone by hydroxyl radial. And in the next step, O_4^- is oxidized by ozone to form O_2. Finally, both O_3^- and O_3^- may be protonated, O_2 molecule being form.

The uptake coefficients γ of NO_x, acetaldehyde and ozone shows that the γ threshold limit value of $1x10^{-5}$ (Ifang et al., 2014) was exceeded in majority cases (SFig. 5B). Especially, at their lower inlet concentrations of 0.1 ppmv, in a wide range of irradiation intensities a high γ values were achieved.

3.3. Photocatalytic degradation of pollutants in mixtures

Based on the degradation mechanisms determined for the separate pollutant, it is reasonable to expect that there will not be a significant interference when they are degraded in a mixture. This hypothesis was verified by an experimental study as follows.

Regarding the photocatalytic degradation of a two-component mixture of acetaldehyde and ozone (SFig. 6A, B), the photocatalytic conversion remained unchanged (roughly 20 per cent for acetaldehyde and 35 per cent for ozone), even if the inlet concentration of acetaldehyde increased ten-times (from 100 ppbv to 1000 ppbv).

Concerning the photocatalytic degradation of three-component mixture of acetaldehyde, ozone and nitric oxide (Fig. 4), the decrease in concentration was roughly 20 per cent for acetaldehyde, 35 per cent for ozone and 50 per cent for nitric oxide, which agrees with those determined for them separately (see Section 3.2). Moreover, it also agrees with data for two-component mixtures as presented above.

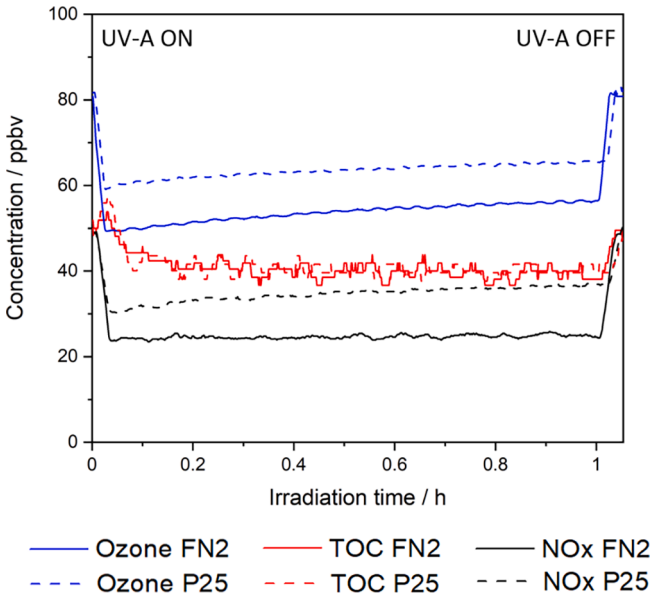

Fig. 4. Photocatalytic abatement of mixture of 50 ppbv acetaldehyde (TOC), 50 ppbv nitric oxide (NOx) and 80 ppbv ozone over FN2 a P25 photocatalytic layers.

The reasonable explanation of non-interference is a different reaction mechanism of individual pollutants. Consequently, there was no competition between them in the mixture and the system behavior was purely additive. This finding is very important from the viewpoint of the application of this technology for the degradation of various types of gaseous pollutants whose nature differs considerably. In the literature, some sort of interference between two pollutants in their simultaneous photocatalytic degradation was reported. The nature of such interference depended on the character of the tested molecules. While in one study [12] an inhibition effect of similar molecules was observed, in another study, a synergistic enhancement occurred [11]. In the latter study, the nature of tested molecules mutually differed (NH_3 and H_2S) and also their chemical features completely differed from those addressed in our study.

The performed study shows that the relationship between the photocatalyst features, and its performance depends on the specific mechanism, by which the respective pollutant is degraded. For nitric oxide, characterized by an important role of adsorption and the formation of deposits, binder-containing FN2 is preferable. Its developed porous structure and high surface area are beneficial for this type of mechanism. On the hand, for acetaldehyde and ozone, these features do not play any role and the performance of both photocatalysts is comparable.

4. Conclusions

The performed experimental study shows more general conclusions as follows. The specificity of the pollutant degradation mechanism may serve as a guide for the right selection of the most suitable photocatalyst, e.g., with or without a binder. Furthermore, the finding that no interference of the selected air pollutants, which represent their most important types, occurred in their photocatalytic degradation in mixtures, enables simplifying the modeling of the photocatalytic process under real-world conditions. Therefore, it is possible to use kinetic data determined for individual pollutants separately to predict the efficiency of the photocatalytic purification of complex pollutant mixtures in the air.

Funding

The research was funded by Ministry of Industry and Trade of the

Czech Republic (Grant No. FV40209) and by Czech Science Foundation for financial support (Grant No. 19-12109S).

CRediT authorship contribution statement

Radek Zouzelka: Conceptualization, Writing – original draft, Writing – review & editing, Validation. **Ivana Martiniakova:** Investigation, Validation. **Tomas Duchacek:** Methodology, Investigation. **Barbora Muzikova:** Investigation. **Eliska Mikyskova:** Investigation, Methodology, Validation. **Jiri Rathousky:** Supervision, Project administration, Funding acquisition, Conceptualization.

Declaration of Competing Interest

The authors declare that they have no known competing financial interests or personal relationships that could have appeared to influence the work reported in this paper.

Data availability

Data will be made available on request.

Acknowledgments

Further, the authors also acknowledge the assistance provided by the Research Infrastructures NanoEnviCz (Project No. LM2018124) supported by the Ministry of Education, Youth and Sports of the Czech Republic and the project Pro-NanoEnviCz (Reg. No. CZ.02.1.01/0.0/0.0/16_013/0001821) supported by the Ministry of Education , Youth and Sports of the Czech Republic and the European Union - European Structural and Investments Funds in the frame of Operational Programme Research Development and Education for providing access to structural determination. Finally, the research was supported by the Academy of Sciences of the Czech Republic within the program Strategy AV21 No. 23 - The City as a Laboratory of Change; buildings, cultural heritage and an environment for a safe and valuable life“.

Appendix A. Supplementary data

Supplementary data to this article can be found online at https://doi.org/10.1016/j.jphotochem.2022.114235.

References

[1] E. Boonen, A. Beeldens, Recent photocatalytic applications for air purification in Belgium, Coatings 4 (2005) 553–573, https://doi.org/10.3390/coatings4030553.
[2] R.W. Cheary, A.A. Coelho, J.P. Cline, Fundamental parameters line profile fitting in laboratory diffractometers, J. Res. Natl. Inst. Stand. Technol. 109 (2004) 1–25, https://doi.org/10.6028/jres.109.002.
[3] B. Dhandapani, S.T. Oyama, ! Paper (1997) - Gas phase ozone decomposition catalysts.pdf, Appl. Catal. B Environ. 11 (1997) 129–166.
[4] M. Gallus, V. Akylas, F. Barmpas, A. Beeldens, E. Boonen, A. Boréave, M. Cazaunau, H. Chen, V. Daële, J.F. Doussin, Y. Dupart, C. Gaimoz, C. George, B. Grosselin, H. Herrmann, S. Ifang, R. Kurtenbach, M. Maille, A. Mellouki, K. Miet, F. Mothes, N. Moussiopoulos, L. Poulain, R. Rabe, P. Zapf, J. Kleffmann, Photocatalytic depollution in the Leopold II tunnel in Brussels: NOx abatement results, Build. Environ. 84 (2015) 125–133, https://doi.org/10.1016/j.buildenv.2014.10.032.
[5] B. Hauchecorne, D. Terrens, S. Verbruggen, J.A. Martens, H. Van Langenhove, K. Demeestere, S. Lenaerts, Elucidating the photocatalytic degradation pathway of acetaldehyde: An FTIR in situ study under atmospheric conditions, Appl. Catal. B Environ. 106 (2011) 630–638, https://doi.org/10.1016/j.apcatb.2011.06.026.
[6] S. Kalathil, M.M. Khan, S.A. Ansari, J. Lee, M.H. Cho, Band gap narrowing of titanium dioxide (TiO_2) nanocrystals by electrochemically active biofilms and their visible light activity, Nanoscale 5 (2013) 6323–6326, https://doi.org/10.1039/c3nr01280h.
[7] S. Laufs, G. Burgeth, W. Duttlinger, R. Kurtenbach, M. Maban, C. Thomas, P. Wiesen, J. Kleffmann, Conversion of nitrogen oxides on commercial photocatalytic dispersion paints, Atmos. Environ. 44 (2010) 2341–2349, https://doi.org/10.1016/j.atmosenv.2010.03.038.
[8] Y. Lu, X. Zhao, M. Wang, Z. Yang, X.J. Zhang, C. Yang, Feasibility analysis on photocatalytic removal of gaseous ozone in aircraft cabins, Build. Environ. 81 (2014) 42–50, https://doi.org/10.1016/j.buildenv.2014.05.024.
[9] T. Maggos, J.G. Bartzis, M. Liakou, C. Gobin, Photocatalytic degradation of NOx gases using TiO_2-containing paint: a real scale study, J. Hazard. Mater. 146 (2007) 668–673, https://doi.org/10.1016/j.jhazmat.2007.04.079.
[10] Maggos, T., Plassais, A., Bartzis, J.G., 2008. Photocatalytic degradation of NOx in a pilot street canyon configuration using TiO_2 -mortar panels 35–44. 10.1007/s10661-007-9722-2.
[11] G. Maxime, A. Aymen Amine, B. Abdelkrim, W. Dominique, Removal of gas-phase ammonia and hydrogen sulfide using photocatalysis, nonthermal plasma, and combined plasma and photocatalysis at pilot scale, Environ. Sci. Pollut. Res. 21 (2014) 13127–13137, https://doi.org/10.1007/s11356-014-3244-6.
[12] J. Palau, A.A. Assadi, J.M. Penya-Roja, A. Bouzaza, D. Wolbert, V. Martínez-Soria, Isovaleraldehyde degradation using UV photocatalytic and dielectric barrier discharge reactors, and their combinations, J. Photochem. Photobiol. A Chem. 299 (2015) 110–117, https://doi.org/10.1016/j.jphotochem.2014.11.013.
[13] H.M. Rietveld, A profile refinement method for nuclear and magnetic structures, J. Appl. Crystallogr. 2 (1969) 65–71, https://doi.org/10.1107/s0021889869006558.
[14] B. Tryba, P. Rychtowski, A. Markowska-Szczupak, J. Przepiórski, Photocatalytic decomposition of acetaldehyde on different tio2-based materials: A review, Catalysts 10 (2020) 1–26, https://doi.org/10.3390/catal10121464.
[15] M.E. Zorn, D.T. Tompkins, W.A. Zeltner, M.A. Anderson, Photocatalytic oxidation of acetone vapor on TiO2/ZrO2 thin films, Appl. Catal. B Environ. 23 (1999) 1–8, https://doi.org/10.1016/S0926-3373(99)00067-3.
[16] R. Zouzelka, J. Rathousky, Photocatalytic abatement of NOx pollutants in the air using commercial functional coating with porous morphology, Appl. Catal. B Environ. 217 (2017) 466–476, https://doi.org/10.1016/j.apcatb.2017.06.009.